Pyrolysis of Polymethylsilsesquioxane

JUN MA,[1] LIANGHE SHI,[1] YONGYXI SHI,[2] SHANGUO LUO,[1] JIAN XU[1]

[1] State Key Laboratory of Polymer Physics & Chemistry, The Center for Molecular Science, Institute of Chemistry, The Chinese Academy of Sciences, Beijing 100080, People's Republic of China

[2] Beijing University of Chemical Technology, Beijing 100029, People's Republic of China

Received 26 March 2001; accepted 8 June 2001

ABSTRACT: Changes of the composition and structure of various samples of polymethylsilsesquioxane (PMSQ), pyrolyzed at different temperatures under flowing nitrogen, were investigated using thermogravimetric analysis, Raman and Fourier transform infrared spectroscopies, X-ray photoelectron spectroscopy, elemental analysis, scanning electron microscopy, and transmission electron microscopy. The center of the Si2*p* peak could be used to estimate the extent of the pyrolysis of PMSQ. Two temperature domains correspond to important changes in the chemical composition of PMSQ. The former ($T_p < 500$°C) is related to the conversion from a regular structure to an irregular structure and the latter ($T_p > 500$°C) is associated with the organic–ceramic conversion. During the latter pyrolysis, flowing of the molten bulk occurred and then a final solid structure was obtained. The main product of PMSQ, pyrolyzed at 900°C, is silica, as well as some amount of silicon oxycarbide and traces of amorphous carbon. Based on the above analysis and observation, a conversion process from polysilsesquioxane to a ceramic is proposed. © 2002 Wiley Periodicals, Inc. J Appl Polym Sci 85: 1077–1086, 2002

Key words: polymethylsilsesquioxane; pyrolysis; ceramic

INTRODUCTION

The term polysilsesquioxanes in this article refers to all structures with the empirical formulae $(RSiO_{3/2})_n$, where R is hydrogen or any alkyl, alkylene, aryl, arylene, or organo-functional derivatives of alkyl, alkylene, aryl, or arylene groups. Since Chi and Baney[1,2] first reported in 1984 the conversion of silsesquioxanes to silicon oxycarbide ceramics, frequently referred to as black glass, the use of polysilsesquioxanes as precursors to silicon oxycarbide ceramics through pyrolysis at elevated temperatures in inert atmospheres has become a very active field of research. Polysilsesquioxanes can serve as easily synthesized precursors to silicon oxycarbides in which silicon, oxygen, and carbon are incorporated into an amorphous network structure. These systems offer promise for applications including matrices,[3] anodes,[4] joints,[5] infiltrates,[6] ceramic films,[7] and coatings in ceramic matrix composites.[8]

Polymethylsilsesquioxane (PMSQ) is characterized by its low weight loss at high temperatures, 800°C, although the initial decomposition temperature is somewhat lower than that of polyphenylsilsesquioxane. Li and Hwang[9] investigated the pyrolysis kinetics of PMSQ using thermogravimetry both under isothermal conditions and by increasing the temperature at 10°C/min.

Correspondence to: J. Ma (mlye@pplas.icas.ac.cn).

Contract grant sponsor: Natural Science Foundation of China; contract grant number: 20074039.

Contract grant sponsor: State Key Laboratory of Polymer Physics and Chemistry; contract grant number: 00-B-01).

Journal of Applied Polymer Science, Vol. 85, 1077–1086 (2002)

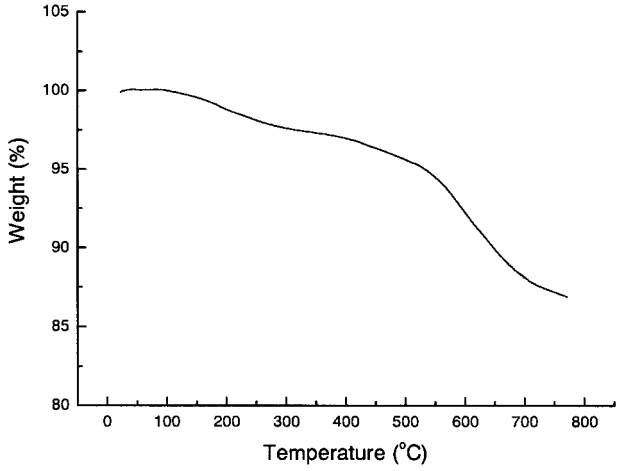

Figure 1 TG traces of PMSQ in N_2, heating rate 10 K/min.

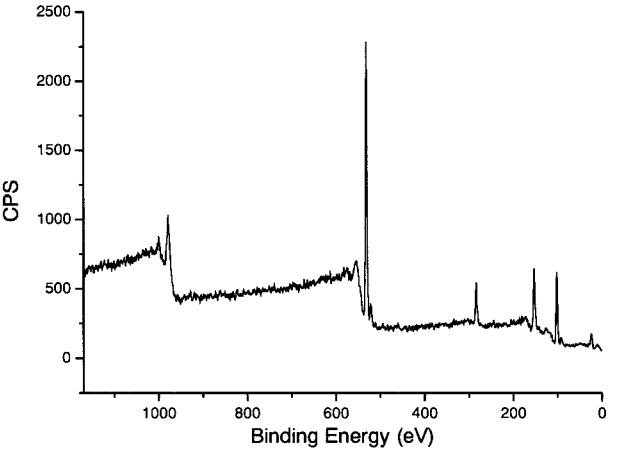

Figure 2 XPS spectrum of PMSQ crosslinked in air and heated treated at 900°C under an inert atmosphere.

^{29}Si-MAS–NMR studies by Belot and Corriu[10] revealed that inert gas pyrolysis of methylsilsesquioxane gels first leads to a loss of methane and hydrogen to about 1000°C and solid-state redistribution of Si—C and Si—O bonds at higher temperatures. However, to our knowledge, X-ray photoelectron spectroscopy (XPS) characterization and microstructure observation of PMSQ were unavailable from the literature mentioned above.

The pyrolysis of PMSQ could be expected to influence the thermal expansion, modulus, and perhaps oxidative stability of the pyrolyzed product. The present work focused on systematically varying the pyrolysis temperature to investigate its influence on the structure of the pyrolyzed PMSQ, as well as characterizing the structure of it. For industrial application, the treatment temperature is often limited to under 1000°C and, hence, in this study, pyrolysis was carried out in an inert atmosphere up to 900°C. The conversion process and intermediate and final products were characterized by thermogravimetric analysis (TGA), Raman and Fourier transform infrared (FTIR) spectroscopies, elemental analysis (EA), X-ray photoelectron spectroscopy (XPS), scanning electron microscopy (SEM), and transmission electron microscopy (TEM).

EXPERIMENTAL

Specimen Preparation

Methyltrimethoxysilane was provided by the Shin-Etsu Chemical Corp. Ltd. (Japan). Silica was purchased from the Beijing Xinxing Chemical Reagent Factory (Beijing, China). Silicone carbide was provided by the United Carbon Corp. PMSQ was synthesized from methyltrimethoxysilanes by hydrolysis/condensation and then crosslinked in air at 80°C for 3 h, as described elsewhere.[11]

Pyrolysis was performed with 2–5 g ground solid PMSQ. The sample was loaded into a carborundum crucible and placed into a carborundum tube furnace over which nitrogen flowed. The samples were heated at a rate of 10 K/min to different pyrolysis temperatures. The obtained pyrolyzed samples (brownish or blackish chunks or powders) were used in the following investigations.

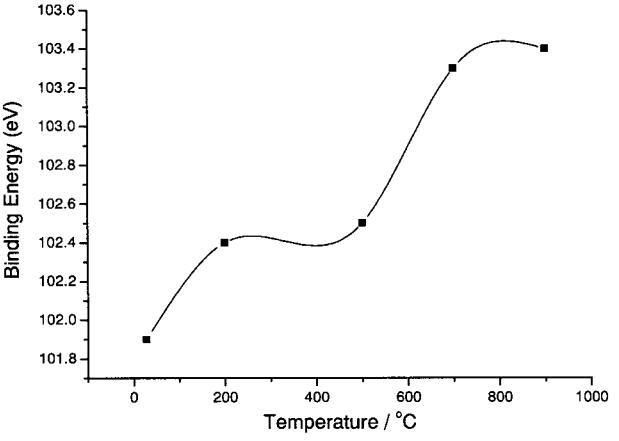

Figure 3 Binding energies of PMSQ pyrolyzed at different temperatures.

Table I Binding Energies (eV) Corresponding to Different Atomic Bonding in Various Materials Containing Silicon

Materials	Si—O (II)	Si(C,O) (III)	Si—C (I)	References
SiO layer on silicon	103.2	102.2	101.1	15
Ex-PCS filament				
Surface	103.2	102.2	101.1	16
Bulk		101.9	100.8	17
CVD SiC	103.4		101.2	18

Chemical Analyses

TGA was conducted in flowing nitrogen (30 cm^3 min^{-1}) at a heating rate of 10°C min^{-1} using a Perkin–Elmer TGA 7. EA of the pyrolyzed materials was performed by a BJST-O2. Carbon and hydrogen were determined by combustion in oxygen using an induction furnace technique and gel chromatography.

The XPS spectra were recorded (ESCALAB 220I-XL XPS spectrometer) with AlKα (1486.6 eV) as the excitation source on the analyzed area of the pyrolyzed material, having a width of about 150 μm and a length of 150 μm. The X-ray source power was 15 kV $\times$ 20 mA. The analyses were performed, under a residual pressure less than 5 $\times$ 10^{-9} mbar, on pyrolyzed material after heat treatment at 200, 500, 700, and 900°C.

Changes in the chemical structure of the coatings were assessed by infrared (FTIR) and Raman spectroscopies. Chunks of the pyrolyzed material were polished to about 0.5 μm dust using diamond pastes. The FTIR spectrum was recorded in transmission from 4000–400 cm^{-1} at 1-cm^{-1} resolution, using a Bruke Equinox 55 FTIR/FRA 106 spectrometer. The Raman data were obtained with an Instruments Bruke FRA 106/S spectrometer. The Raman spectra were collected using a DILOR X–Y microspectrometer fitted with a Ge detector in flowing argon and the bandpass was 4 cm^{-1}. The laser excitation source was the 1.06-μm line of a YAG laser, operated at 150 mW, and the beam was rastered over 75 μm.

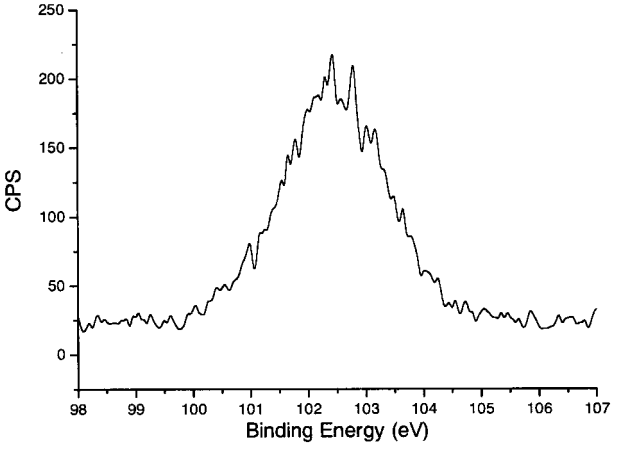

Figure 4 Si2*p* peak of XPS spectrum of PMSQ pyrolyzed at 200°C.

Microstructural Observation

The nano- and microstructural features of the heat-treated PMSQ were derived from SEM and TEM analyses. Specimens for TEM were prepared from bulk material by standard techniques of grinding, polishing, and dimpling to thicknesses less than 40 μm and then were examined using an H-800 transmission microscope.

For SEM characterization, fracture surfaces were prepared at room temperature and examined after they had been coated with a thin gold coating using a GIKO IB-3 ION coater. To avoid distortion of the polymer surface, we chose a coating temperature of 40°C by moderating the number and time of coating under a low electric current and high voltage. Micrographs were obtained at magnifications ranging from 1000 to 10,000 using a Hitachi S-530 SEM.

Table II Binding Energies (eV) Derived from the XPS Peaks in Heat-treated PMSQ at Different Stages of Pyrolysis

PMSQ Treatment	Si2*p*		
	Si—O (II)	Si(C,O) (III)	Si—C (I)
At 200°C	103.4	102.5	101.4
At 500°C	103.5	102.6	101.3
At 700°C	103.4	102.4	
At 900°C	103.5	102.3	

Table III Quantitative XPS Analysis of the Chemical Bonds (at %) at Different Stages of Pyrolysis

	Si2*p*		
Materials	Si—O (II)	Si(C,O) (III)	Si—C (I)
At 200°C	21.6	60.1	18.3
At 500°C	13.2	72.0	14.9
At 700°C	89.4	10.6	
At 900°C	91.6	8.4	

RESULTS AND DISCUSSION

Chemical Change During PMSQ Pyrolysis

As shown in Figure 1, the TGA curve of the pyrolyzed PMSQ sample, performed after the crosslinking step, suggests that two important conversions occur in the material as temperature is increased, below and above 500°C. The former results in a weight loss of 4.25%. The first step in the weight loss begins almost immediately on heating, with the maximum rate of loss occurring at about 100°C. This is attributed to the evolution of continued condensation of silanol and the reaction of methoxide groups. An overlapping weight loss is observed in the region at about 200°C, which corresponds to the loss of low molecular weight cyclic PMSQ structures.[12] At this point, the sample is still colorless and transparent. The latter conversion takes place at higher temperatures, $T_p > 500$°C. Severe decomposition reactions take place in this range, which gradually darken the sample. It results in a marked decrease in its carbon content (which decreases from 8.6 to 1.7%, derived from EA) and some decrease in PMSQ weight (from 95.7 to 87.1%). The weight decrease in this conversion centered at 540–650°C is attributed to evolution of CO, and that at 700–750°C, to evolution of CH_4.[13] Less weight loss is observed above 750°C. It has been reported that between 800 and 1400°C weight loss is limited to <1.5% and probably reflects the evolution of hydrogen from Si—CH_2—Si linkages which incorporate into the backbone by redistribution reactions.[10,13,14]

XPS analyses, performed at different stages of pyrolysis, showed that all materials are made of silicon (Si2*s* and Si2*p* peaks), carbon (1*s* peak), and oxygen (1*s* peak), as illustrated in Figure 2 for the pyrolytic residue obtained at 900°C. It is well known that peak positions for XPS data vary somewhat from instrument to instrument. Thus, authentic samples of silica (SiO_2) and silicone carbide (SiC) were run to confirm peak positions. Si2*p* binding energies of SiO_2 and SiC are 103.1 and 100.1 eV, respectively.

As shown in Figure 3, the center of the Si2*p* peak was plotted against the pyrolysis temperature starting with unpyrolyzed PMSQ to that pyrolyzed at 900°C. A significant increase of Si2*p* energy from room temperature to 200°C was observed, which could be caused by the condensation of silanol, reaction of the methoxide groups, and loss of low molecular weight cyclic PMSQ structures. A smaller increase of Si2*p* energy from 200 to 500°C might hint at less reaction in this range. Above 500°C, the value increased sharply to 103.3 eV, which is very similar to the 103.1 eV of silica tested in this research. This

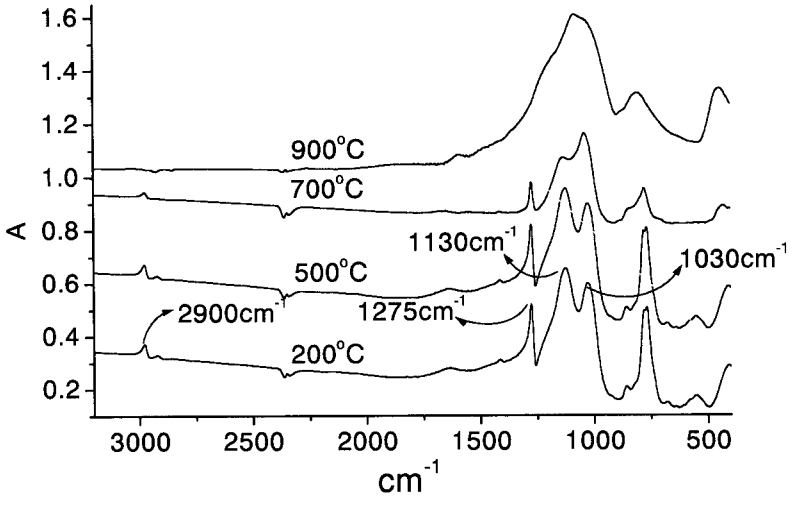

Figure 5 FTIR spectroscopy of PMSQ heated at different temperatures.

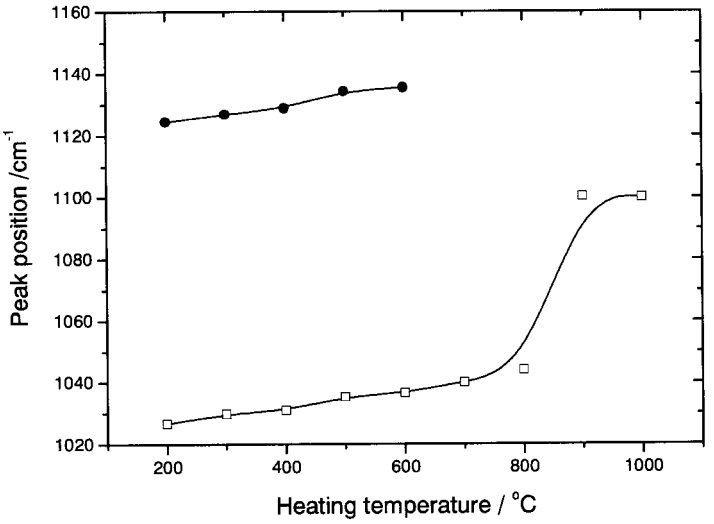

Figure 6 Changes of the IR absorption peak due to Si—O—Si stretching vibration for pyrolyzed PMSQ with heating temperature.

conclusion proves that the center of the Si2*p* peak would be useful in estimating the extent of PMSQ pyrolysis.

Deconvolution is a useful procedure to study the components of pyrolyzed polysiloxane. Several previous results are listed in Table I, which shows that the Si2*p* peak consists of two or three components. In this article, the curve of the Si2*p* binding energy is plotted in Figure 4, from which obvious shoulder peaks at 101 and 103 eV are found. Compared with the 100.1 and 103.1 eV of SiC and SiO_2, respectively, the 102 shoulder peak might correspond to local structures of $CSiO_3$, C_2SiO_2, and so on. Therefore, the deconvolution process of Si2*p* was conducted based on the obvious shoulder peaks at 101 and 103 eV. Generally, deconvolution is based on the concept that there are distinct species. In this study, however, what exists are only continuous compositions from SiO_2 to SiC. The following three energy values correspond to different chemical bonds in the process of pyrolysis, instead of distinct species. This deconvolution method was used by several researchers.[16,17] The energy values corresponding to the various chemical bonds, derived from the XPS peaks (recorded in the high-resolution mode), are listed in Table II. The first (I) at about 101 eV is assigned to Si—C bonds, whereas the second (II) at about 103 eV is assigned to Si—O bonds. Finally, a third component (III) at about 102 eV for the polymeric materials, which first increases and then decreases as pyrolysis proceeds toward the ceramic state, is also observed between those corresponding to Si—C and Si—O bonds. It is assigned to a ternary Si (C,O) species. A similar component was also reported recently.[15–17,19,22]

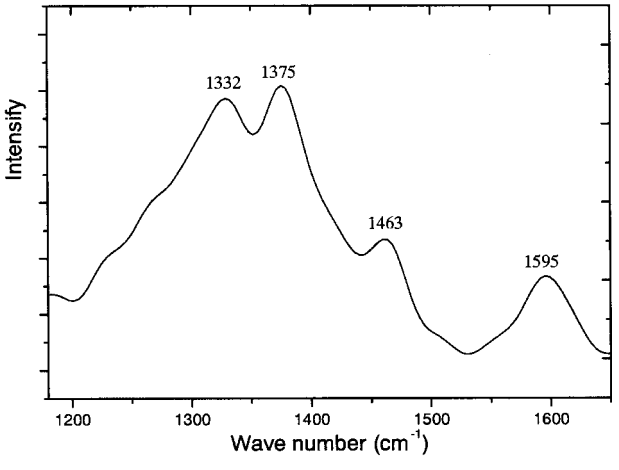

Figure 7 Raman spectra of PMSQ pyrolyzed at 900°C.

A quantitative analysis of the components of the Si2*p* peak in the materials at different steps of the PMSQ heat treatment is given in Table III. It shows that two temperature domains correspond to important changes in the chemical composition of PMSQ: (i) $T_p < 500$°C and (ii) $T_p > 500$°C. The former is related to the conversion from a regular structure to an irregular structure and the latter is thought to be associated with the organic–ceramic conversion. From 200 to 500°C, the values of Si–O and Si–C decrease, but that of Si(C,O) increases. Some researchers report that polysilsesquioxanes embrace a regular ladderlike structure.[23,24] It appears that heat treatment in this temperature range makes the structure more ir-

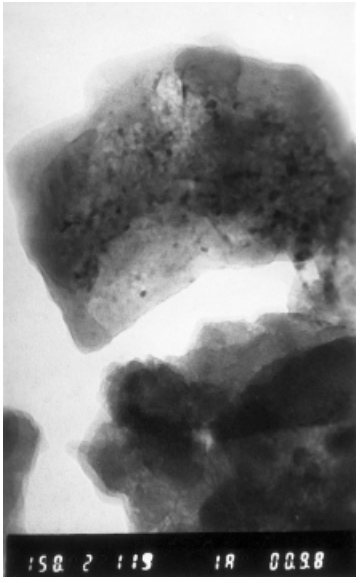

Figure 8 Bright-field TEM image of PMSQ pyrolyzed to 900°C in nitrogen.

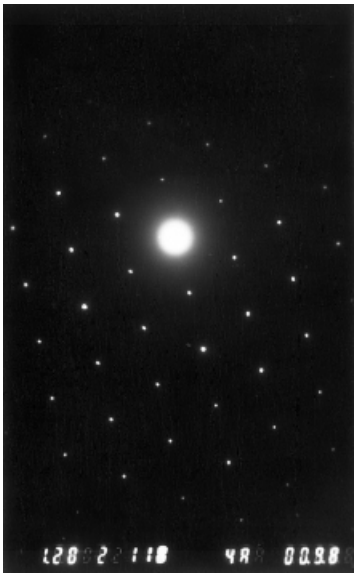

Figure 10 Selected-area diffraction of PMSQ pyrolyzed to 900°C in nitrogen.

regular. During the organic–ceramic conversion at 500–900°C, the percentage of Si—O increases substantially, but that of Si(C,O) decreases excessively. It proves that the main component of the final pyrolyzed product might be SiO_2. The data also show that materials heat-treated at 700 and 900°C are almost free of Si–C.

Infrared spectra over the wavenumber range from 400 to 4000 cm^{-1} of the pyrolyzed PMSQ heated in N_2 are shown in Figure 5. The bands at 3400 and 1600 cm^{-1} are OH vibrations derived from the KBr. The absorption bands at around 2900 cm^{-1} belong to the C—H vibrations of —CH, —CH_2 and —CH_3 groups. The methyl groups (CH_3) are also characterized by absorption bands of 1410 and 1275 cm^{-1}, respectively. The Si–CH_3 band intensity decreases with an increasing heat-treatment temperature. The band decomposed around 700°C and disappeared completely at 900°C, which corresponds to XPS analyses. Typical polysilsesquioxane absorption bands are at 1030 and 1130 cm^{-1}, corresponding to the regularity of ladderlike polysilsesquioxane.[24–26] With increase of the pyrolysis temperature, the band

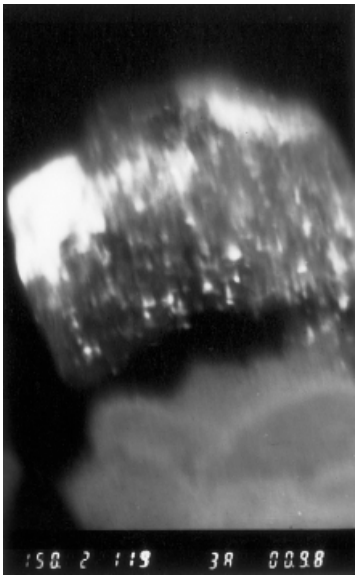

Figure 9 Dark-field TEM image of PMSQ pyrolyzed to 900°C in nitrogen.

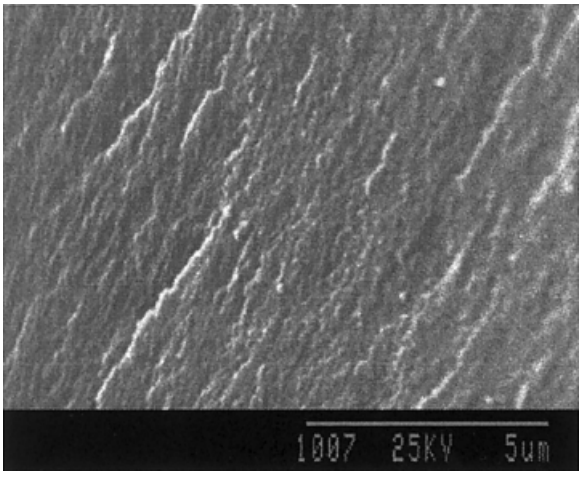

Figure 11 SEM micrographs of fracture surface heat-treated at 200°C.

intensity of 1130 cm^{-1} decreases, but the band intensity of 1030 cm^{-1} increases, which indicated an increase of irregularity of the PMSQ structure. At 900°C, the two bands disappear and are replaced by a strong and large absorption band at 1100 cm^{-1}. This large band is similar to that of SiO_2,[27] which is in good agreement with the XPS results. In Figure 6, the wavenumber of the absorption peak due to the Si—O—Si stretching vibration at 1000–1100 cm^{-1} is plotted against the heating temperature. The pyrolyzed PMSQ shows a gradual increase in the wavenumber of the peak due to Si—O bonding as the heating temperature is increased and reached the value for SiO_2 glass at 900–1000°C. It seems that organic groups gradually disappear with increasing temperature.

Although the C,H analysis no longer shows any hydrogen content for this product, the IR spectrum, as one can see from the CH absorption band at around 2900 cm^{-1}, still proves a residual H content bound to carbon, which is in good agreement with Schneider.[12] It can be explained by FTIR having higher resolution than that of EA.

Raman spectroscopy was used to analyze more accurately free carbon in these materials. The Raman spectra of PMSQ in this study are dominated by four bands in Figure 7. The spectrum of microcrystalline graphite exhibits two bands, at well-defined energies of 1355 and 1580 cm^{-1}, the latter shifting up to 1620 cm^{-1} in nanocrystalline or turbostratic graphite, while both bands shift toward each other in amorphous carbon.[28] The higher the degree of sp^3 hybridization, the stronger is this shift, until forming a single feature centered at 1520–1540 cm^{-1} in the most diamondlike films. The 1355-cm^{-1} mode is due to an in-plane zone-edge phonon that is symmetry-forbidden for one-phonon Raman scattering. However, when the graphite crystallite size is small enough, the wave vector conservation selection rule applicable to large crystals is relaxed and Raman scattering from this phonon is observed.[29]

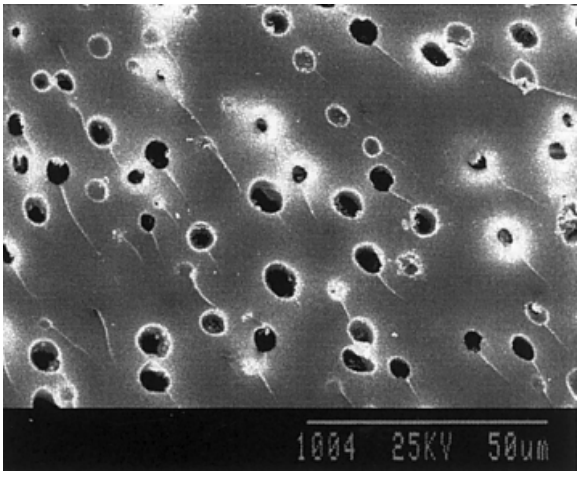

Figure 12 SEM micrographs of fracture surface heat-treated at 500°C.

As shown in Figure 7, PMSQ processed at 900°C has a band at approximately 1332 cm^{-1}, which is strong evidence for sp^3-bonded carbon, a relatively large shift from the normal carbon A_{1g} band that appears around 1354 cm^{-1}. Amorphous sp^3 carbon should have a significant intensity at approximately 1300 cm^{-1}.[30] The shift in frequency above 1595 cm^{-1} from the normal position at 1580 cm^{-1} is another manifestation of the relaxation of the wave vector conservation selection rule due to crystallite size effects or defects. Contributions to Raman scattering from phonons near the peak in the one-phonon density of states just below the zone-boundary phonon at 1620 cm^{-1} (forbidden in Raman scattering from large, single-crystal graphite) cause an apparent shift to higher frequency for the 1580-cm^{-1} mode.[31,32] The Raman band at 1375 cm^{-1} appears very near the frequencies characteristic of sp^2-bounded carbon, which is similar to those reported by Hurwitz et al.[13] and other authors,[32,33] during the pyrolytic conversion of polysilsesquioxanes to silicon oxycarbide. The shift from sp^3 to sp^2 carbon also causes the Raman band at 1460 cm^{-1}, which shows there still exists some amorphous carbon in the sample.

Structural Change During PMSQ Pyrolysis

TEM can be used effectively to assess crystallinity as well as homogeneity and phase distribution in pyrolyzed polymers. The techniques employed are bright-field imaging, dark-field imaging, and selected-area diffraction. The material was ground and suspended on carbon films which were fixed on copper grids. Bright-field images revealed a particle size of approximately 1 nm in all specimens pyrolyzed at 900°C as shown in Figure 8. These particles are confirmed to be amorphous in dark-field images, as shown in Figure 9. However, such particles could not be found in TEM images of other specimens pyrolyzed at 200, 500, and 700°C. In fact, samples gradually darkened during the second process, which shows that this process gives rise to carbon particles. From Raman analysis, the particles should be amorphous carbon. As shown in Figure 10, bulk material was found to be fine crystals. Based on XPS quantitative analysis, the bulk should be silicon.

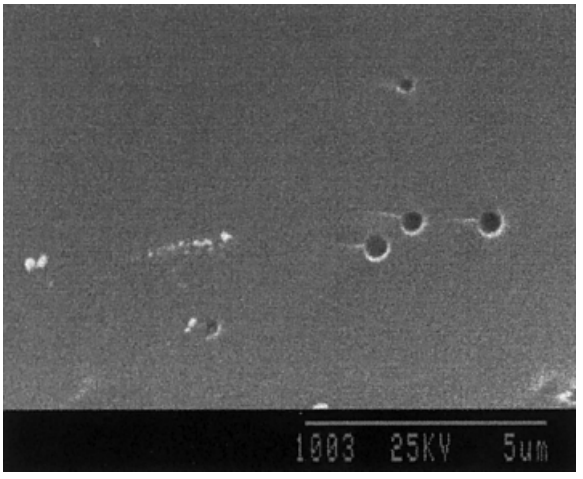

Figure 13 SEM micrographs of fracture surface heat-treated at 700°C.

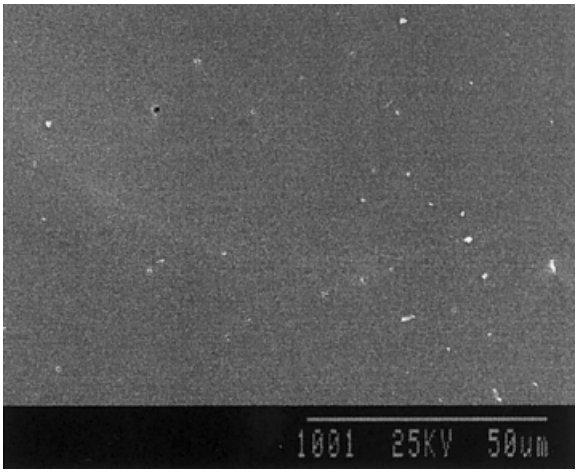

Figure 14 SEM micrographs of fracture surface heat-treated at 900°C.

By SEM investigation, the difference in the microstructures of PMSQ heat-treated at different temperatures under flowing nitrogen was observed from fractured surfaces. Figure 11 shows the surface of the sample treated at 200°C. It is found that the sample has a solid structure without any holes or particles. Figure 12 shows the surface of the sample treated at 500°C. It was found that there are many spherical holes on the surface with an approximate diameter of 3 μm. This is expected because some gases, such as H_2O and CH_3OH, are given off during the processing. Figure 13 shows that the surface of the sample treated at 700°C has a decreased number and size of holes. Figure 14 shows the solid surface structure again. It can be explained that, with increase of temperature, the amount of released gas becomes smaller and there still exists flowing of molten bulk in the process of pyrolysis and, hence, these holes are filled. As a matter of fact, we obtained solid pyrolyzed PMSQ with a reduced volume at the end of heat treatment.

Conversion Process from Polysilsesquioxane to Ceramic

In the first pyrolysis stage ($T_p < 500$°C) of PMSQ, weight loss occurs due to dehydrogenation and evaporation of the low molecular weight components. During the second stage ($T_p > 500$°C), dehydrocarbonation condensation occurs. The main reaction occurring during the pyrolysis of organic polymers at this stage is generally free radical in nature. With an increasing heat-treatment temperature, redistribution of Si—O and Si—C occurs, which has been mentioned by several authors.[21,34–37] Based on the analysis of FTIR and XPS spectra, the main final component of pyrolyzed PMSQ should be SiO_2. Thus, the primary reactions in the decomposition is assumed to be as follows:

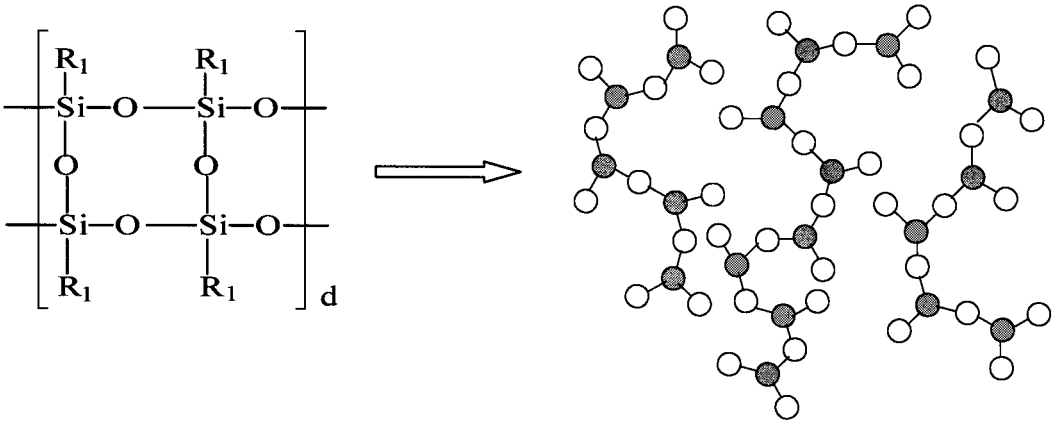

However, FTIR analysis shows traces of hydrogen content. The cleavage of the Si—C bonds occurred with the loss of hydrocarbons, as reported by some researchers,[38–40] but the Si—C bond is relatively stable toward homolytic fission under free-radical reaction conditions, whereas the C—H bonds in Si—CH_3 are readily broken. The formation of methane occurs as follows:

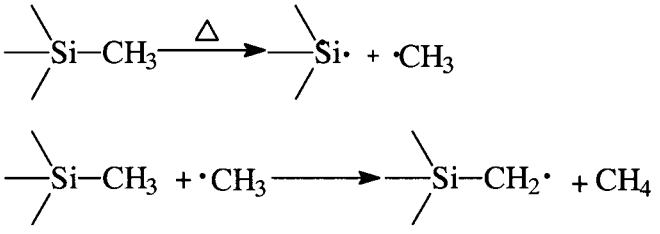

Recombination of the radicals produced in the above equations can also lead to the formation of Si—CH_2—Si bonds and Si—CH—Si bonds,[41] as well as to CH_4 as shown below:

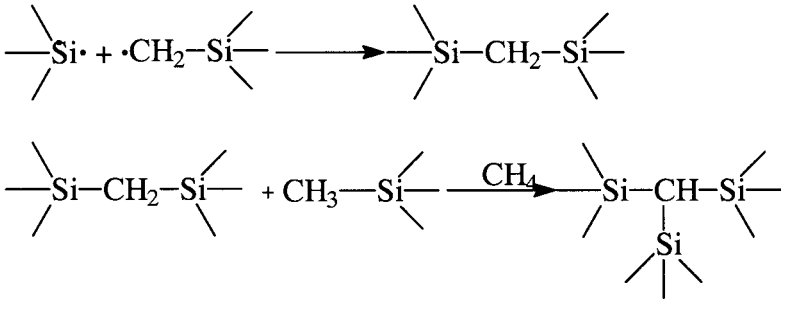

The above CH and CH_2 correspond to the CH-absorption band at around 2900 cm^{-1} in the FTIR spectra.

CONCLUSIONS

The current work indicates that the main component of PMSQ pyrolyzed at 900°C is silica, as well as some amount of silicon oxycarbon and traces of carbon. XPS shows that two temperature domains correspond to an important change in the chemical composition of the PMSQ: (i) $T_p < 500$°C and (ii) $T_p > 500$°C. The former is related to the conversion from a regular structure to an irregular structure and the latter is thought to be associated with the organic–ceramic conversion. The center of the Si2*p* peak could be used to estimate the extent of pyrolysis of PMSQ. The changes in the chemical composition are explained in the light of the quantitative analysis of the chemical bonds.

Characterization of the conversion process in FTIR shows that with increase of the temperature Si—C cleavage occurs and the band at the wavenumber of the absorption peak due to Si—O—Si stretching at 1000–1100 cm^{-1} changes regularly. The spectra of the sample pyrolyzed at 900°C are similar to those of SiO_2. FTIR analysis shows traces of hydrogen content.

The microstructure of the fracture surface of PMSQ pyrolyzed at different temperatures was observed by SEM. It shows that some amount of gases were given off and the total volume decreased during the pyrolysis. In the second conversion, some melt-flowing of the bulk occurred and, therefore, a final solid structure was obtained. Based on the above analysis and observation, a conversion process from polysilsesquioxane to ceramic is proposed.

This project was supported by the Natural Science Foundation of China (No. 20074039) and State Key Laboratory of Polymer Physics and Chemistry (N0.00-B-01).

REFERENCES

1. Chi, F. K. Ceram Eng Sci Proc 1983, 4, 704.
2. Baney, R. H.; Chi, G. K. Eur Patent 107 943.

3. Haluska, L. A.; Michael, K. W. Eur Patent Appl EP 750 337 A2, Dec. 27, 1996.
4. Zank, G. A. Jpn Patent 11 130 539 A2, May 18, 1999 (to Heisei).
5. Colombo, P.; Riccardi, B.; Donato, A.; Scarinci, G. J Nucl Mater 2000, 278, 127.
6. Li, D.; Hwang, S. T. J Membr Sci 1991, 59, 331.
7. Takamura, N.; Taguchi, K.; Gunji, T.; Abe, Y. J Sol–Gel Sci Technol 1999, 16, 227.
8. Camilletti, R. C.; Haluska, L. A.; Michael, K. W. Eur Patent Appl EP 834 489 A, Apr. 18, 1998.
9. Li, D.; Hwang, S. T. J Appl Polym Sci 1992, 44, 1979.
10. Belot, V.; Corriu, R. J Polym Sci Lett 1990, 9, 1052.
11. Ma, J.; Xu, J. Chin Patent 130 514 X.
12. Schneider, O. Thermochim Acta 1988, 134, 269.
13. Hurwitz, F.; Heimann, I. P.; Farmer, S. C.; Hembree, D. M. J Mater Sci 1993, 28, 6622.
14. Laine, R. M.; Rahn, J. A.; Youngdahl, K. A.; Basonneau, F.; Hoppe, M. L.; Zhang, Z. F.; Harrod, J. F. Chem Mater 1990, 2, 464.
15. Taylor, J. A. Appl Surf Sci 1981, 7, 168.
16. Bouillon, E.; Mocaer, D.; Villeneuve, J. F. J Mater Sci 1991, 26, 1517.
17. Porte, L.; Sartre, A. J Mater Sci 1989, 2, 271.
18. Mizokawa, Y.; Geib, K. M.; Wilmsed, C. W. J Vac Technol A 1986, 4, 1696.
19. Lipowitz, J.; Freeman, H. A.; Chen, R. T.; Prack, E. R. Adv Ceram Mater 1987, 2, 121.
20. Laffon, C.; Flank, A. M.; Hagege, R.; Olry, P.; Cotteret, J. J Mater Sci 1989, 24, 1503.
21. Wager, C. D. Handbook of X-ray Photoelectron Spectroscopy; Perkin–Elmer Corp. Physical Electronics Division: 6509 Flying Clound Dr., Eden Prairie, MN, 1979, Part 52.
22. Aswyer, L. C.; Chen, R. T.; Haimback, F.; Harget, P. J. Ceram Eng Sci Proc 1986, 7, 914.
23. Brown, J. F., Jr.; Vogt, J. H., Jr.; Katchman, A.; Eustance, J. W.; Kiser, K. M.; Krantz, K. W. J Am Chem Soc 1960, 82, 6194.
24. Zhang, X. S.; Shi, L. H. Chin J Polym Sci 1987, 5, 359.
25. Li, G. Z.; Shi, L. H.; Ye, M. L. Chin J Polym Sci 1996, 14, 41.
26. Xie, Z. S.; He, Z. Q.; Dai, X. R.; Zhang, R. B. Chin J Polym Sci 1989, 7, 183.
27. Atlas of Polymer and Plastics Analysis, Vol. 3, Additives and Processing Aids, Spectra and Methods of Identification, Friedrich Scholl: Germany.
28. Pivin, J. C.; Colombo, P. J Mater Sci 1997, 32, 6163.
29. Tuinstra, F.; Koenig, J. L. J Chem Phys 1970, 53, 1126.
30. Wada, N.; Gaczi, P. J.; Solin, S. A. J Non-Cryst Solids 1980, 35–36, 543.
31. Knight, D. S.; White, W. B. J Mater Res 1989, 4, 385.
32. Nemanich, R. J.; Solin, S. A. Phys Rev B 1979, 20, 392.
33. Day, R. J.; Piddock, B.; Taylor, R.; Young, R. J.; Zakikhani, M. J Mater Sci 1989, 24, 2898.
34. Wagener, G. H.; Pines, A. N. Ind Eng Chem 1952, 4, 321.
35. Chubarov, V. A.; Nasenkis, M. A.; Zher, Y. V.; Korolec, A. Y.; Avrasin, Y. D.; Andrianov, K. A. Polym Sci USSR 1973, 15, 2981.
36. Zhang, X. S.; Shi, L. H.; Li, S.; Lin, Y. Polym Degrad Stab 1988, 20, 157.
37. Kamiya, K.; Ohya, M.; Yoko, T. J Non-Crystal Solids 19896, 83, 208.
38. Hasegawa, Y.; Okamura, K. J Mater Sci 1983, 18, 3633.
39. Singh, A. K.; Pantano, C. G. J Sol-Gel Sci Technol 1997, 8, 371.
40. Corriu, R. J. P.; Leclercq, D.; Mutin, P. H.; Vuoux, A. J Sol-Gel Sci Technol 1997, 8, 327.
41. Soraru, G. D. J Sol-Gel Sci Technol 1994, 2, 843.